Before the
FEDERAL COMMUNICATIONS COMMISSION
Washington, D.C. 20554

In the Matter of ANSYS, Inc. Request for Waiver of Section 1.1307(b)(2) of the Commission's Rules	)	OET Docket No. 10-166

REPLY COMMENTS OF ANSYS, INC.

ANSYS, Inc., but its undersigned counsel, submits these reply comments in support of its request to the Commission for waiver of Section 1.1307(b)(2) of the Commission's Rules, 47 C.F.R. § 1.1307(b)(2), to permit routine environmental evaluation of medical implant or body-worn equipment authorized for use in the Medical Device Radiocommunication (MedRadio) Service by finite element method (FEM) computational modeling. That rule currently restricts routine environmental evaluation for RF exposure of equipment transmitting in the MedRadio Service to actual laboratory measurement techniques or finite difference time domain (FDTD) computational modeling. The effect of the rule as written is to prohibit reliance on any alternative simulation modeling techniques, including FEM and, as a result, Ansys' proprietary FEM-based software tool, High Frequency Structure Simulator ("HFSS").

In its request for waiver filed with the Commission on August 2, 2010, ANSYS provided scientific literature in support of its arguments that FEM is capable of simulating fundamental physics identical to that of FDTD while operating on a different but equally valid technical basis,[1] and that FEM is recognized and utilized in the industry as a simulation modeling

[1] ANSYS, Inc. request for waiver, at 1-2.

technique of equivalent credibility to FDTD.[2] ANSYS also demonstrated that the Commission's adoption of Section 1.1307(b)(2) to restrict reliance on computational modeling in the evaluation of MedRadio Service transmitting equipment to FDTD was based on a deficient record, and that perpetuating enforcement of the rule's restrictive nature causes unnecessary economic harm to ANSYS and to the marketing of its proprietary FEM-based software, HFSS.[3] Finally, ANSYS explained that both FDTD and FEM are awaiting formal acceptance by the IEEE Standards Committee, and cannot be differentiated in the rules from one another on that basis.[4]

The Commission put ANSYS' request for waiver on public notice for comment on August 24, 2010.[5] Significantly, no comments have been received by the Commission in opposition to ANSYS' request, and none of the premises underlying ANSYS' request to advance the public interest through grant of its waiver have been rebutted.

The only comment received in response to the Commission's Public Notice supports the scientific basis for ANSYS' waiver request. Cambridge Consultants, Inc., which supports outsourced wireless and medical product development, utilizes ANSYS' HFSS modeling software on its antenna systems designs, including those developed as implantable devices for use in the MedRadio Service. From Cambridge Consultants' informed perspective, FEM and FDTD yield "nearly identical data, making either [simulation modeling] method equivalent for evaluating RF exposure."[6] In support of its argument that FEM and FDTD should be considered equally valid and effective simulation methodologies for equipment authorization purposes,

---

[2] *Id.*, at 2.

[3] *Id.*, at 3.

[4] *Id.*

[5] DA 10-1600, released August 24, 2010.

[6] Comments of Cambridge Consultants, Inc., September 21, 2010, at 2.

Cambridge Consultants cites two scientific studies. Copies of these articles have been attached for the Commission's convenience and information as Attachments 1 and 2. In Attachment 1,[7] Figure 4 in particular depicts how closely the results of the FEM and FDTD methodologies track one another. In Attachment 2,[8] the input impedance of, and the coupling between, cavity-backed slot antennas are computed using both FDTD and FEM. The results are compared in figures 2 and 3. Again, the authors of the paper conclude that the results of the two methodologies agree very well.

In conclusion, the record in this proceeding contains solid evidence that FEM is as scientifically legitimate and effective a simulation modeling technique as FDTD for routine environmental evaluation of medical implant or body-worn equipment authorized by the Commission. The Commission's grant of ANSYS' requested waiver will, therefore, advance the purpose of Section 1.1307(b)(2) and the public interest. In addition, approval of the waiver request will rectify the current inequitable treatment of ANSYS and other users of FEM technology and will implement Section 1.1307(b)(2) in a more technologically neutral fashion. The record in this proceeding demonstrates that FEM represents an equally sound technical solution to fulfill the public purpose for which the use of FDTD modeling was originally recognized in the Commission's rules. Therefore, special circumstances warrant deviating from the general rule in the public interest, as proposed by ANSYS.

---

[7] A. Bhobe, C. Holloway, and M. Picket-May, "Meander Delay Line Challenge Problem: A comparison using FDTD, FEM and MOM," *IEEE International Symposium on Electromagnetic Compatibility*, vol. 2, pp. 805-10, August 2001.

[8] S. Georgakopoulos, A. Polycarpou, C. Balanis and C. Birtcher, "Analysis of Coupling Between Cavity-Backed Slot Antennas: FDTD, FEM & Measurements," *IEEE Antennas and Propagation Society International Symposium*, vol. 1, pp. 582-85, July 1999.

For all the foregoing reasons, the Commission should approve without further delay ANSYS' request for waiver of Section 1.1307(b)(2).

Respectfully submitted,

ANSYS, INC.

By: Delbert D. Smith

Delbert D. Smith
Jones Day
51 Louisiana Avenue, N.W.
Washington, D.C. 20001-2113
(202)879-7600
Its Counsel

October 8, 2010

ATTACHMENT 1

Meander Delay Line Challenge Problem: A comparison using FDTD, FEM and MoM*

Alpesh U. Bhobe
University of Colorado at Boulder, Department of Electrical Engineering
Campus Box 425, Boulder, CO 80309

Christopher L. Holloway
National Institute of Standards and Technology (NIST)
U.S. Department of Commerce, Boulder Laboratories
325 Broadway, Boulder, CO 80303

Melinda Piket-May
University of Colorado at Boulder, Department of Electrical Engineering
Campus Box 425, Boulder, CO 80309

Abstract: Full-wave finite-difference time-domain (FDTD) and a simplified 1D- finite-difference time-domain technique using the multi-conductor transmission line equations were applied to a delay line to determine its propagation characteristics. The output voltage waveform was calculated using the two methods and the results were compared to those obtained by two commercially available finite-element codes and two method-of-moment codes. Radiated fields from this structure are also included for the different numerical approaches.

I. INTRODUCTION

In recent years, the IEEE EMC Society's TC-9 committee (Computational Electromagnetics Technical Activities Committee) has identified specific EMC problems that have certain features that would aid the validation and delineation of the practical limits of different numerical modeling techniques. These problems are referred to as "real-world challenge problems." One such problem, which is the topic of this paper, is the meander delay line shown in Fig. 1. In this paper various numerical techniques are used to analyze the delay line in order to address the focus of this TC-9 activity.

Delay lines are used in printed-circuit boards (PCB) in computer systems. The popular delay lines are the meander (Fig. 1.) and the spiral delay line. In meander lines, distortion of the output waveform depends on the separation between the adjacent segments. If the segments are close to each other, the mutual coupling increases, which causes distortion that might cause false switching of logic gates [1]-[3]. If the separation distance is increased, the overall area containing the line increases, which is undesirable. The mutual coupling causes the pulse to arrive at the output faster than expected.

In order to study how the meander line functions, both time and frequency domain characteristics of the structure must be considered. When a signal propagates through a transmission line, commonly referred to as a PCB trace, the mode of transmission is electromagnetic waves. Maxwell's equations must be solved to determine the characteristics of these waves.

A variety of methods have been developed for numerical solution of partial differential equations and of integral equations. Numerical studies in electromagnetics have resulted in the development of improved and powerful methods [4]-[8]. These full-wave techniques include finite-difference time-domain (FDTD), finite-element method (FEM) and method of moments (MoM).

In this paper we apply the full-wave FDTD technique and a simplified 1D-FDTD technique to the meander delay line. We compare the output waveforms generated and the delay obtained using the two methods. We then compare these results to the results obtained from two different commercially available FEM and MoM codes. From here onwards, we will refer to these codes as FEMa, FEMb, MoMa and MoMb, respectively. We will also compare the run time performance of each code.

0-7803-6569-0/01/$10.00 © 2001 IEEE

In our study we examine the following:

1. Effects on signal propagation in the time domain
2. Frequency domain characteristics of the meander line
3. Radiated emissions at different frequencies

This paper is organized in the following way. Section II describes the geometry of the meander line under study. Sections III, IV, V and VI briefly introduce the numerical techniques (3D-FDTD, 1D-FDTD, FEM, and MoM) used to analyze the meander line propagation characteristics. Section VII discusses the numerical results.

II. Description of The Delay Line Structure

The delay line considered for study is a meander (or serpentine) delay line. The geometry of the line is shown in Fig. 1. The delay line is composed of 8 meander segments and is designed to have a total length of 177 mm. The adjacent segments are separated by 1 mm. Each line has a width of 1 mm. The traces are placed on a 1mm thick dielectric material with relative permittivity 4.5 that has a ground plane on the other side. The characteristic impedance of the line is 71 ohms. The pulse source has a quasi-square (boxcar) pulse shape. The leading and falling edges of the pulse are approximated by gaussian functions with 200 ps rise and fall times. The full dwell time is 1 ns.

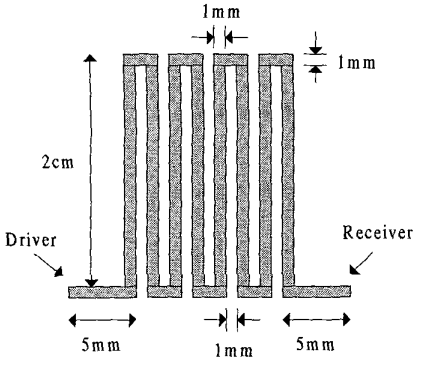

Fig. 1. Top view of the delay Line

III. Finite-Difference Time-Domain Method (FDTD)

The FDTD technique, as introduced by Yee [9], has been proven to be a convenient and effective tool for time-domain analysis of various electromagnetic scattering problems involving arbitrarily shaped objects. The method has been used by authors in electromagnetic pulse coupling [10]. The FDTD method makes use of the increased power of today's computers to provide full time-domain solutions. The basis of the FDTD algorithm is the two time-domain Maxwell's curl equations. These equations are expressed in discrete form by means of central finite differencing.

For uniform, isotropic and homogenous media Maxwell's curl equations are given as

$$\nabla \times \mathbf{E} = -\mu \frac{\partial \mathbf{H}}{\partial t} \tag{1a}$$

$$\nabla \times \mathbf{H} = \sigma \mathbf{E} + \varepsilon \frac{\partial \mathbf{E}}{\partial t}, \tag{1b}$$

where **E**, **H**, ε, μ, and σ are the electric field, magnetic field, permittivity, permeability, and conductivity, respectively. The central difference approximation is used on both the time and space first-order partial differentiations in order to obtain discrete approximations, which gives [9]

$$H^{n+1/2}_{x(i,j+1,k+1)} = H^{n-1/2}_{x(i,j+1,k+1)} + \frac{\Delta t}{\mu \Delta z}\left[E^{n}_{y(i,j+1,k+1)} - E^{n}_{y(i,j+1,k)}\right] - \frac{\Delta t}{\mu \Delta y}\left[E^{n}_{z(i+1,j,k+1)} - E^{n}_{z(i-1,j,k+1)}\right] \tag{2}$$

for H_x and similar equations for the E_x, E_y, E_z, H_y and H_z components.

The permittivity and the permeability are set to the approximate values depending on the location of each field component. Half time steps indicate that E and H fields are alternately calculated in order to achieve central differences for the time derivatives. This results in six equations similar to the one given above. These equations define the E and H fields in the x, y and z directions. After calculating the time-domain E and H fields, the data are transformed into the frequency domain using a fast Fourier transform (FFT).

The finite-difference algorithm requires that the time increment Δt, has a specific bound relative to the grid sizes Δx, Δy, Δz. This bound is necessary to avoid numerical instabilities. The maximum time step that may be used, is limited by the stability restriction of the finite-difference equations, is given by;

$$\Delta t < \frac{1}{v_{\max}}\left[\frac{1}{\Delta x^2} + \frac{1}{\Delta y^2} + \frac{1}{\Delta z^2}\right]^{-1/2}, \tag{4}$$

where $v_{max} = (1/\mu\varepsilon)^{1/2}$ is the maximum speed of the electromagnetic wave in the material being modeled.

The computation region of the FDTD method must be limited in size. This region must be large enough to enclose the structure being modeled. Within the outer boundary, Maxwell's equations are solved in their finite-difference form. However, these equations cannot be implemented along their outer boundary because they allow propagation of waves in all directions and also employ a central-difference scheme that requires knowledge of the fields one half-cell to each side of the point where the central-difference approximations are applied. Hence, the basic equations used inside the numerical domain must be modified on the outer boundary. The most commonly used absorbing boundary conditions are the second-order condition derived by Mur [11] and perfectly matched layer (PML) derived by Berenger [12].

IV. 1-D FDTD For Multiconductor Transmission Line Method

In this method, a finite-difference time-domain algorithm is applied to the multi-conductor transmission line (MTL) equations [13]-[14]. The voltages and currents on an n+1 conductor MTL are described by the coupled partial differential equations

$$\frac{\partial}{\partial x}V(x,t)+L\frac{\partial}{\partial t}I(x,t)+RI=V^s(x,t) \tag{5}$$

$$-\frac{\partial}{\partial x}I(x,t)+C\frac{\partial}{\partial t}V(x,t)+GV=I^s(x,t), \tag{6}$$

where $V(x, t)$ and $I(x, t)$ are the column vectors of the n voltages and currents on the MTL, and $V^s(x, t)$ and $I^s(x, t)$ are the column vectors of the n distributed voltage and current sources produced by, for instance, an external electromagnetic field. The $n \times n$ matrices L, R, C and G are the per unit length inductance, resistance, capacitance, and conductance matrices describing the MTL. In order to mutually integrate the transmission line equations, we use the finite-difference technique. When the central-difference technique is used, the numerical solution results in the following equations:

$$I_i^{n+1/2}=[A]\cdot[LRT]\left[I_i^{n-1/2}\right]-\frac{[A]}{\Delta x}\left\{\left[V_{i+1}^n\right]-\left[V_i^n\right]\right\}+[A]\left[V^s\right] \tag{7}$$

$$V_i^{n+1}=[B]\cdot[CGT]\left[V_i^n\right]-\frac{[B]}{\Delta x}\left\{\left[I_{i+1}^{n+1/2}\right]-\left[I_i^{n+1/2}\right]\right\}, \tag{8}$$

where the index i indicates the spatial location and the index n indicates the time location, and

$$[A]=\left[\frac{[L]}{\Delta t}+\frac{[R]}{2}\right]^{-1} \qquad [B]=\left[\frac{[C]}{\Delta t}+\frac{[G]}{2}\right]^{-1} \tag{9}$$

$$[LRT]=\left[\frac{[L]}{\Delta t}-\frac{[R]}{2}\right]^{-1} \qquad [CGT]=\left[\frac{[C]}{\Delta t}-\frac{[G]}{2}\right]^{-1}. \tag{10}$$

Note that V and I are always offset by one half of a time step and half of a spatial step. The finite-difference equation first advances all the currents on the transmission line one-time step based on the voltages at the previous time step. Then the voltages are advanced by using the currents that were just calculated. For stability of this scheme, one needs to ensure that:

$$\Delta t<\frac{\Delta x}{v},$$

where Δt is the time step, Δx is the spatial cell size, and v is the velocity of propagation on the line. This criterion is usually referred to as the Courant stability condition and essentially states that the numerical speed of propagation must exceed the physical speed of propagation. Note that there are no radiation effects captured from the 1-D FDTD formulation.

V. Method of Moments

The Method of Moments (MoM) is essentially the method of weighted residuals [5], which can be used for solving both differential and integral equations. The use of MoM in electromagnetics (EM) has become popular since the work of Richmond [15] in 1965 and Harrington [16] in 1967. The method has been successfully applied to wide variety of EM problems of practical interest such as radiation due to thin-wire elements and arrays, scattering problems, and the analysis of microstrip and lossy structures.

The procedure for applying MoM to electromagnetic problems usually involves four steps:

- Derivation of the appropriate integral equation
- Conversion (discretization) of the integral equation into a matrix equation
- Evaluation of the matrix elements, and
- Solving the matrix equation and obtaining the parameters of interest.

VI. Finite-Element Method

The finite-element method has its origin in the field of structural analysis. Although the earlier mathematical treatment of the method was provided by Courant [17] in 1943, the method was not applied to electromagnetic problems until 1968. Although MoM and FDTD techniques are conceptually simpler and easier to implement numerically, the FEM is a more versatile and powerful technique for handling problems involving complex geometries and inhomogeneous media. The starting point of the finite-element method (FEM) is the subdivision of the domain into small sub-domains called elements. Although the elements need not be triangles, those subdivisions are called a triangulation. An element is described by its vertices and one point on each edge. These points are called the nodes. The FEM mesh is constituted by its nodes and the elements. Equilateral triangles (or tetrahedra) work best for the 2^{nd}-order interpolation functions between nodes. The approximation is calculated on the nodes of the elements, which is sufficient to approximate the fields at any point. The problem is to find the values of the solution approximation at the nodes of the FEM mesh from the given PDE. Thus, the original boundary-value problem with an infinite number of degrees of freedom is converted into a problem with a finite number of degrees of freedom; or in other words, the solution of the whole system is approximated by a finite number of unknown coefficients. The basic steps are:

- Discretization or subdivision of the domain
- Selection of the interpolation functions
- Formulation of the system of equations
- Solution of the system of equations.

VII. Numerical Modeling and Results

The FDTD method was first used to model the meander delay line. A uniform grid with cells of dimension $\Delta x = \Delta y = \Delta z = 0.25$ mm was used. The dimension was chosen to give a cell resolution of approximately 95 cells per wavelength at the highest frequency corresponding to the rise time of the source waveform. The substrate was modeled as a dielectric with relative permittivity of 4.5 and dimensions 26 mm × 26 mm × 1 mm. The meander line was placed over the dielectric and a ground plane on its other side. Overall, the computational space was 104 × 104 × 20 cells, for 216320 total cells. The time step was 4.13×10^{-13} seconds. The computational domain was truncated using PML that was 8 cells deep. A source with a Gaussian rising and falling edge of 200 ps and a dwell time of 1 ns was used. The source has excitation frequency content up to 15 GHz. Both, the source line and the receiver line were truncated into the PML. The source and the receiving probes were placed 10 cells away from the PML to avoid ringing effects due to the PML. A total of 12000 time steps were used in simulations.

A similar approach was applied to the 1D-FDTD method. A resolution of 40 cells per wavelength at 15 GHz was used. The source waveform used was similar to that used in the 3D-FDTD simulations. The right-angled bends were modeled using lumped elements.

The same line was modeled in FEMa, FEMb, MoMa and MoMb. In FEM modeling, an air box of the dimension of 23 mm × 41 mm × 30 mm was created. The dielectric, of dimension 23 mm × 41 mm × 1 mm, was placed on the lower face of the air box, on which a perfect conductor boundary condition is defined. Thus the lower face acts a ground plane to the trace. The input and output traces run into the two opposite faces of the air box. These two faces are defined as the ports. In each port, a vertical impedance line is created between the center of the trace and the bottom of the ground plane. With an impedance line at the port, the voltage difference between the signal trace and the ground plane is determined by integrating the electric field along the line. Perfect conductor boundary conditions are defined on the traces by forcing the tangential electric field on the surface to equal zero. Radiation boundary conditions are defined on the remaining faces of the air box. The radiation boundaries model surfaces that represent free space. Electric and magnetic fields are allowed to travel through the boundaries instead of being contained within them.

MoM solvers, being planar circuit full-wave solvers, can enable easier set-up of the meander line problem as compared to their FEM counterparts. The steps involved are:

1. Creating a physical design of the meander line
2. Defining the substrate characteristics, which included the number of layers in the substrate and the position of the layer of the meander line

3. Solving the substrate for a range of frequencies from 1 to 15 GHz. This approximates the Green's function that characterizes the substrate for the specified range
4. Specifying input and output ports on input and output lines, respectively. Each port was assigned a port impedance of 71 ohms.

The output waveforms obtained from the two FDTD methods are shown in Fig. 2 along with the output waveform from a straight line (non-meandered). The output waveform, delayed by the propagation time through the line, starts rising about 1 ns after the source pulse was launched. The agreement between the two results is in general good. The output wave arrives earlier than expected. This is due to the speed-up effects caused by the mutual coupling between the segments of the meander line.

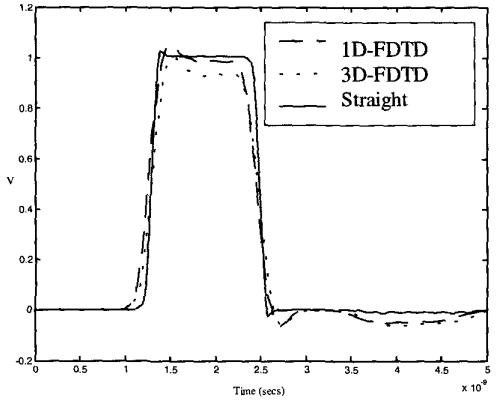

Fig. 2. Output Voltages calculated by the two finite-difference time-domain methods

In both the FEM and MoM codes, 30 cells per wavelength at 5 GHz, were used to discretize the meander line. The solutions were calculated in the frequency domain and converted to the time domain through appropriate inverse Fourier transforms. The results are plotted in Figs. 3 and 4. The results show good correlation with those obtained from the FDTD methods except that the FEM pulses arrive faster than the others.

The magnitude of the reflection coefficient (S_{11}) generated by FDTD-3D, FEMb and MoMb methods are plotted in Fig. 5 for the frequencies between 0.5 and 5 GHz. Again, the results are in good agreement with each other. From the plot, we can conclude that the meander line has good transmission characteristics below frequency of 3.1 GHz, but the performance deteriorates after that until around 4.4 GHz. From these observations, we conclude that, in addition to acting as a delay line, the meander line is well suited for filtering applications. This is true because the spacing and the number of segments control the pass-band corner frequencies and slopes, respectively. This is a well-known characteristic of periodic structures in general.

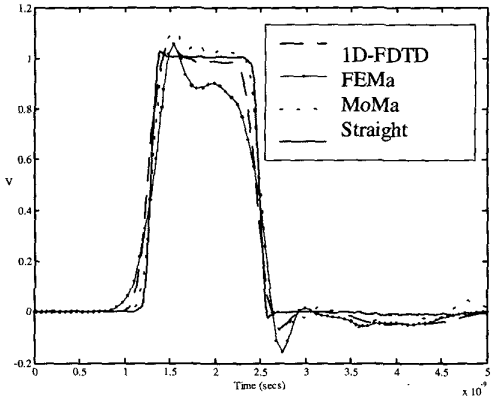

Fig. 3. Comparison of the output voltages calculated by 1-D FDTD, FEMa, MoMa to the straight-line case

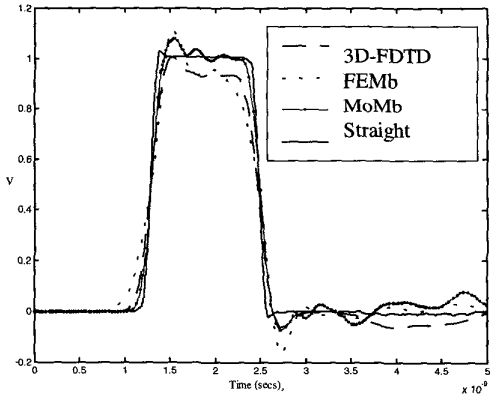

Fig. 4. Comparison of the output voltages calculated by3-D FDTD, FEMa, MoMa to the straight-line case

The magnitude of total electric field 2 cm above the center of the board is shown in Fig. 6. The results obtained are in good agreement. The radiation at this point increases with frequency until 3.4 GHz and then decreases.

The performance of the codes are compared in Table 1. Notice that all the full-wave approaches have approximately the same total run time, with the exception of that for the MoMb.

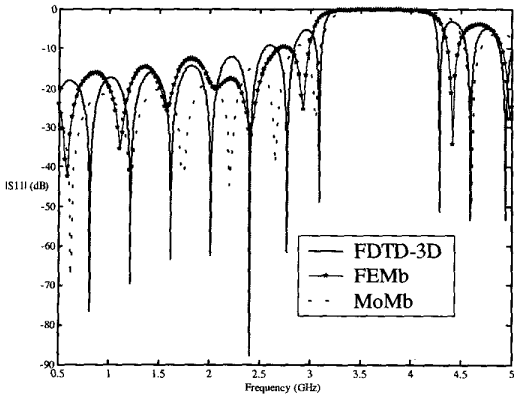

Fig. 5. Comparison of S_{11} calculated by 3D-FDTD, FEMb and MoMb

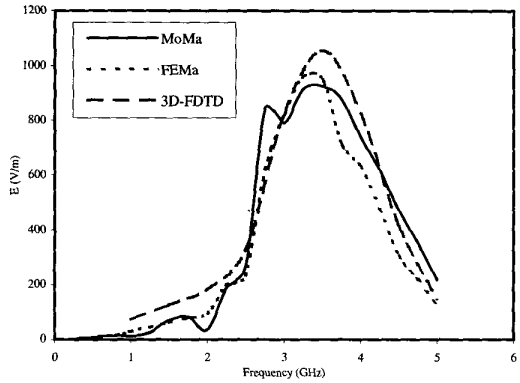

Fig. 6. Comparison of E-field magnitude at a point 2 cm above the meander line

Table 1. Performance comparisons of FDTD, FEM and MoM

Code	Size (MB)	Time (secs) per frequency point	Total Run time (201 points)
FDTD-1D	0.065	-	20mins
FDTD-3D	27.32	-	1hr 33mins
FEMa	19.7	27	1hr 37mins
FEMb	18.472	22.3	1hr 15mins
MoMa	16.8	21	1hr 10mins
MoMb	18.3	57	3hrs 18mins

VIII. CONCLUSION:

A full-wave FDTD and a simplified 1D-FDTD model have been used to analyze meander delay line. Both models take into account the mutual coupling between the adjacent segments of the delay line, and also the right-angled bend effects. The results obtained were compared to those obtained by commercially available FEM and MoM solvers. In all cases the output waveform matched reasonably well. The subtle difference in results using the full-wave approaches is not fully understood and will be the topic of future investigation. The interesting result of the paper is that a simple 1-D transmission line could predict reasonably well the propagation characteristics of the meander line compared to the full-wave approaches.

IX. REFERENCES

[1] B. J. Rubin and B. Singh, "Study of meander line delay in circuit boards," *IEEE Trans. Microwave Theory Tech.*, vol. 48, pp. 1452-1460, Sep. 2000.

[2] R. Wu and F. Chao, "Laddering wave in serpentine delay line," *IEEE Trans. Compon. Packag., Manufact. Technol.*, vol. 18, pp. 644-650, Nov. 1995.

[3] R. Wu and F. Chao, "Flat spiral delay line design with minimum crosstalk penalty," *IEEE Trans. Compon. Packag., Manufact. Techno.*, vol. 19, pp. 397-401, May. 1999.

[4] T. Itoh, *Numerical Techniques for Microwave and Millimeter-Wave Passive Structures*. New York: J. Wiley, 1989.

[5] J. J. H. Wang, *Generalized Moment Methods in Electromagnetics: Formulation and Computer Solution of Integral Equations*. New York. J. Wiley, 1991.

[6] J. Jin, *The Finite Element Method in Electromagnetics*. New York: John Wiley, 1993

[7] M. Sadiku, *Numerical Techniques in Electromagnetics*. Boca Raton, FL. CRC Press, 1992

[8] A. Taflove, *Computational Electrodynamics: the Finite-Difference Time-Domain Method*. Boston: Artech House, 1995.

[9] K. S. Yee " Numerical Solution of initial boundary value problem in solving Maxwell's equations in isotropic media," *IEEE Trans. Antennas Propagation*, vol. AP-14, pp. 302-307, May 1966

[10] R. Holland, L. Simpson, and K. S. Kunz, " Finite-difference analysis of EMP coupling to lossy dielectric structures," *IEEE Trans. Electromagn. Compat.*, vol. 22, pp. 88-97, May 1981

[11] G. Mur, "Absorbing boundary conditions for the finite-difference approximation of the time-domain electromagnetic field equations," *IEEE Trans. Electromagn. Compat.*, vol. 23, pp. 377-382, Nov 1981.

[12] J. P. Berenger, "A perfectly matched layer for the absorption of electromagnetics waves," *J. Computational Phys.*, vol. 114, pp. 185-200, 1994.

[13] C. L. Holloway, "*Numerical simulation of multiple cable multi-branched cables: theory and user manual*," EMA-93-R-003, EMA, Inc., Lakewood, CO, 1992.

[14] C. R. Paul, Analysis of Multiconductor Transmission lines. N.Y., John Wiley, 1994.

[15] J. H. Richmond, "Digital computer solutions of the rigorous equations for scattering problems," *Proc., IEEE*, vol. 53, pp. 796-804, Aug. 1965.

[16] R. F. Harrington, "Matrix methods for field problems," *Proc. IEEE* vol. 55, no. 2, pp. 136-149, Feb. 1967.

[17] R. Courant, "Variational methods for he solution of problems of equilibrium and vibrations," *Bull. Am. Math. Soc.*, vol. 49, pp. 1-23, 1943.

ATTACHMENT 2

Analysis of Coupling between Cavity-Backed Slot Antennas: FDTD, FEM & Measurements

Stavros V. Georgakopoulos*, Anastasis C. Polycarpou,
Constantine A. Balanis and Craig Birtcher
Department of Electrical Engineering
Telecommunications Research Center
Arizona State University
Tempe, AZ 85287-7206

1 Introduction

Cavity-backed slot antennas have been widely used in different types of applications within the microwave band, including radars, satellite communications, mobile telephony, broadcast TV, and aircraft/spacecraft communications. They are relatively easy to manufacture, lightweight and often small in size. Their low profile is an important characteristic, especially for aircraft, missile and spacecraft applications, because they can be flush-mounted on the surface of airborne vehicles without affecting the vehicle's aerodynamic profile.

In this paper, the coupling of cavity-backed slot antennas is analyzed by using the finite-difference time-domain (FDTD) method and the finite element method (FEM). Also, parametric studies are performed to examine the dependence of coupling on the frequency of operation and the separation between the apertures. The numerical results are validated by comparison with measurements.

Coupling is an important factor in today's communication systems which have become more complex and use a large number of antennas to support all required services. The reliability and integrity of communication systems can be significantly affected by coupling between transmitting and/or receiving elements, which are mounted on the same structure such as a helicopter or an aircraft airframe. Especially, when a large number of antennas is collocated on the same structure of finite dimensions, interference can deteriorate the quality of communications and corrupt the signals with noise. In addition, airborne communications require extremely reliable systems that sustain continuous operation without jamming or interruption. In such airborne communication systems, the installation of a new antenna appears to be a challenging task. Its mounting location is influenced not only by the type of service the antenna will provide, but also by the mounting locations of the already existing antennas on the airframe. Therefore, the interaction between the new antenna and other radiating elements should be analyzed in order to optimize its position such that coupling satisfies specific requirements. It can be concluded that coupling mechanisms are very important in the design of reliable communication systems.

0-7803-5639-X/99/$10.00 ©1999 IEEE.

2 Analysis and Results

Initially, in order to validate both the FDTD and FEM calculations, an air-filled cavity-backed slot antenna is analyzed. A three-dimensional (3-D) view of the cavity under consideration and a detailed description of the geometry is shown in Figure 1. In the experiment, the aperture antenna was mounted on a finite ground plane of dimensions 24×24 in. and the sharp edges were covered with absorbing material to reduce diffractions. Moreover, the input impedance of the same aperture mounted on an infinite ground plane was calculated in [1] using a hybridization of the FEM with the Moment Method (MM) and compared very well with measurements. It was also shown that the dimensions of the ground plane do not have a profound effect on the value of the input impedance. In the FDTD simulations, this aperture antenna was mounted on a 9×9 cm finite ground plane, which was chosen smaller than the one used in the measurements to avoid a large computational space. The cavity was excited using a voltage source with an internal resistance in order to reduce the computational time. Three different feed methods were used. In all the cases, the feeding probe was excited by a voltage source with R_s equal to 50 ohms. In the first case, the radius of the probe was not modeled (infinitely thin probe) and the cell size was 1.5 mm. In the second case, the radius was taken into account by using the thin-wire model and the cell size was 1.5 mm. Finally, in the third case, the cell size was 0.6 mm and the probe itself was discretized along with the rest of the geometry. Figure 2 illustrates the computed input resistance and reactance of the aperture antenna for the three different cases. Also, the FDTD calculations are compared with measurements and with the results based on the hybrid FEM/MoM formulation which were reported in [1]. Obviously, the accuracy of the FDTD results depends greatly on the wire modeling of the probe that excites the antenna. Excellent agreement between the FDTD computations and the measurements is observed in the case where the probe was discretized. The improvement in accuracy for the last case can be attributed to the finer discretization and the enhanced modeling of the probe.

After, computing the input impedance of the cavity-backed slot antenna, the coupling between two identical cavity-backed slot antennas (whose specifications are defined in Figure 1) mounted on a square 9×9 cm ground plane was computed by FDTD and FEM and the results of the two methods compare very well (see Figure 3 for the geometry specifications and the coupling calculations). The discrepancies at the higher end of the band can be attributed to discretization errors.

Furthermore, parametric studies of the coupling between the two cavity-backed slot antennas shown in Figure 4 were performed both numerically and experimentally; d denotes the separation between the two apertures of the antennas. A sample of these results is illustrated in Figures 5 and 6, where the measured coupling of the two antennas is plotted either versus frequency or separation. It is observed that the coupling between the two antennas diminishes at approximately the same rate as a function of aperture separation at a given frequency.

References

[1] A. Polycarpou, *Finite-Element Analysis of Microwave Passive Devices and Ferrite Tuned Antennas.* PhD thesis, Arizona State University, 1998.

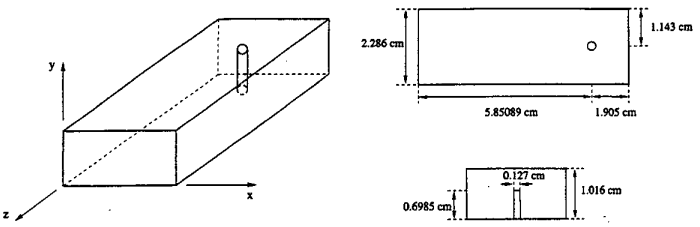

Figure 1: Geometry of a cavity-backed slot antenna fed with a probe in the y-direction.

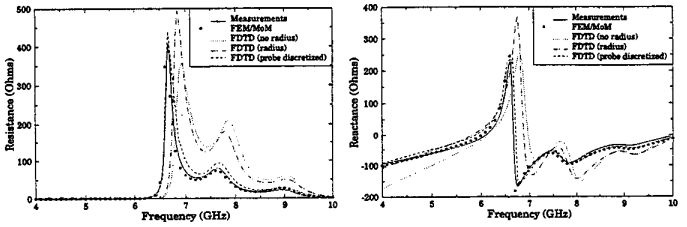

Figure 2: Impedance of a cavity-backed slot antenna (for antenna specifications see Figure 1).

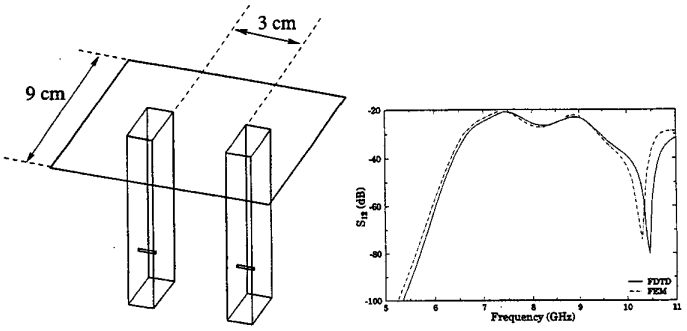

Figure 3: Coupling between two identical cavity-backed slot antennas mounted on a square ground plane (for antenna specifications see Figure 1).

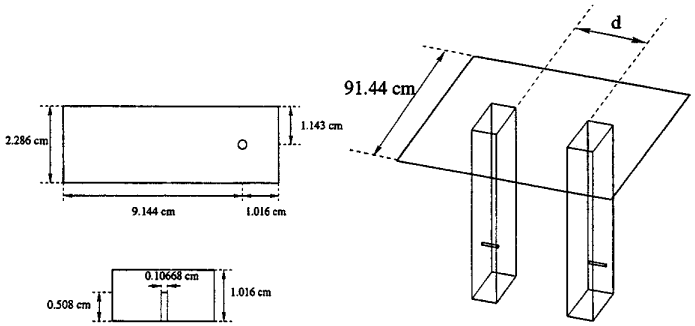

Figure 4: Geometry of two identical cavity-backed slot antennas mounted on a square ground plane along with antenna specifications.

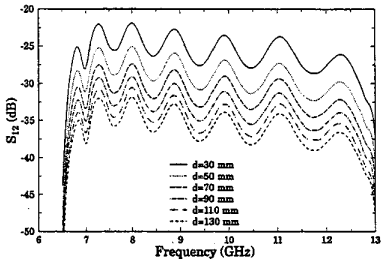

Figure 5: Measured coupling between two cavity-backed slot antennas versus frequency (for antenna specifications see Figure 4).

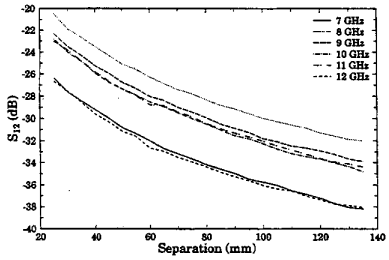

Figure 6: Measured coupling between two cavity-backed slot antennas versus aperture separation (for antenna specifications see Figure 4).